2023 IEEE International Conference on Robotics and Automation (ICRA 2023)
May 29 - June 2, 2023. London, UK

Compliant microgripper using soft polymer actuator

Jung-Hwan Youn[1,2], Je-sung Koh[3], *Member, IEEE,* and Ki-Uk Kyung[1], *Member, IEEE*

***Abstract*— Miniaturization of robotic grippers enables precise manipulation of small-size objects. However, most microgrippers are actuated by rigid actuators, and thus retain challenges such as micro-fabrication, complex structure, and lack of compliance. Here, we present a compliant microgripper driven by a soft polymer actuator. The proposed millimeter-scale soft polymer actuator can produce a linear displacement and output force with a fast operation. Then, we designed the gripper linkage to convert the linear displacement of the actuator into a gripping motion. Fabricated compliant microgripper has a size of 10 × 10 × 10 mm^3 and a weight of 0.36 g, with a maximum gripping width of 8 mm. Demonstration of the gripper shows the feasibility of gripping various sub-millimeter scale objects regardless of their shape owing to its compliance.**

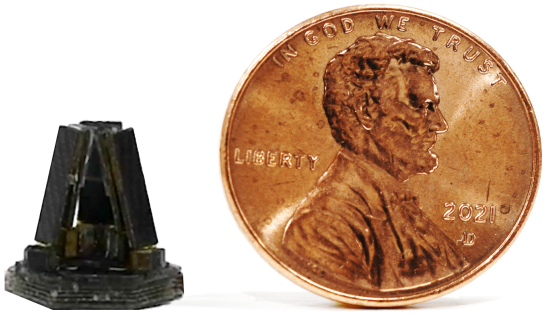

Fig. 1. Fabricated compliant microgripper using soft polymer actuator.

I. Introduction

Over the years, manufacturing technology development has led to a trend toward miniaturized devices that can access and operate in confined and challenging environments. Among such devices, microgrippers play important roles in micro-manipulation, micro-assembly, drug delivery, and minimally invasive surgery [1], [2]. In general, the microgrippers consist of a motion transmission mechanism, actuator, and gripper jaw [3]. To develop microgrippers, transmission linkages, and gripper jaws were successfully fabricated using microelectromechanical system (MEMS) process technology [1]–[4]. Due to the limitations of the silicon micromachining process, the most common microgrippers have a two-dimensional (2D) parallel jaw gripper design [5].

The actuator selection for the microgripper is one of the key design considerations. The actuators suitable for microgrippers should have a small and compact structure and produce sufficient force and displacement with a high resolution. Conventional microgrippers commonly use piezoelectric materials as actuators because such materials facilitate compact size, large output force, high resolution, and fast response speed [2]–[4]. However, the piezoelectric-based microgrippers produce limited gripping width, due to the small displacement of piezoelectric materials. In addition, the rigidity of piezoelectric material makes it difficult to manipulate objects without damage [6]. Various researchers use additional compliant mechanisms to achieve safe grasping [6], [7]. Additionally, the compliance of such microgrippers enables them to grasp various objects without the need for precise feedback control. Although using compliant mechanisms is common in the field of microgrippers, these compliant mechanisms add bulk, complexity, and cost to the system [8]. To overcome these challenges, microgrippers adopted soft actuation principles to enable conformal contact and delicate grasping without extra compliant structures. Several researchers presented compliant microgrippers using various soft actuation principles, such as magnetically driven [9], pneumatically driven [10], and thermally activated polymers [11], shape memory alloy (SMA) springs [12], and electroactive polymers (EAPs) [13], [14]. Although many researchers presented the potential of using soft actuators for microgrippers, several challenges remain. For example, pneumatically-driven grippers require extra components such as pumps or check valves, which makes the overall structure bulky [10]. Thermally activated polymers or SMA spring-based microgrippers operate at high temperatures and have low controllability and slow response time, making them unsuitable for many applications [11], [12]. EAP-based grippers can produce a limited grasping force [13], [14].

Dielectric elastomer actuators (DEAs) are one of EAP-type actuators that exhibit large area strain, fast response, high specific energy density, and low power consumption [15]. Although several soft grippers were developed using DEAs [16], [17], the size and design of the grippers were not suitable for micro manipulation. Research has led to the design of miniaturized DEAs that are suitable for various micro robots, especially microgrippers. Among various DEA configurations, the conical DEA structure has several advantages of producing high output force and large displacement in a single direction [18]–[21]. Typical conical DEAs use a compressive spring [18] or a passive membrane [19]–[21] to pre-stretch a DE membrane. However, compressive spring-

*This research was supported by the Research and Development Program of National Research Foundation (NRF), South Korea, under Grant 2022R1A2B5B02002074 and by internal grant of Electronics and Telecommunications Research Institute (ETRI) [22YS1200] *(Corresponding author: Ki-Uk Kyung)*

[1]Korea Advanced Institute of Science and Technology, South Korea {jungwhan0810, kyungku}@kaist.ac.kr
[2]Electronics and Telecommunications Research Institute, South Korea jungwhan0810@etri.re.kr
[3]Ajou University, South Korea jskoh@ajou.ac.kr

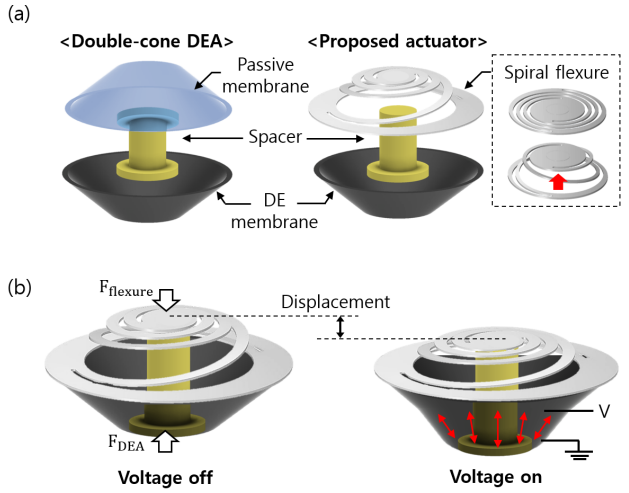

Fig. 2. (a) Design comparison between double-cone DEA and proposed actuator. (b) A working principle of proposed actuator.

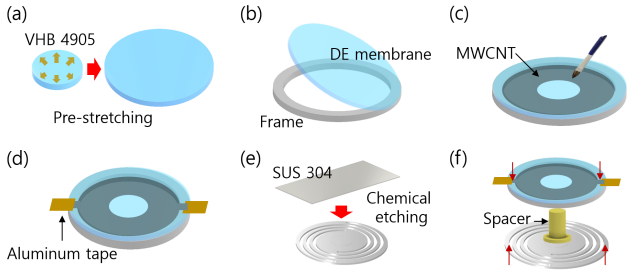

Fig. 3. Fabrication process of actuator: (a) Pre-stretching of DE membrane; (b) attachment of DE membrane to frame; (c) painting of compliant electrodes on both sides of DE membrane; and (d) adding of electrical connection. a-d processes were repeated three times for multi-layer stacking. (e) Chemical etching of stainless steel sheet to make spiral flexure. (f) Place a spacer between membrane and spiral flexure and combine elements.

based conical DEAs have an instability problem due to buckling of the spring; they are also hard to reduce their size. The passive membrane-based conical DEAs, which are also known as double cone DEAs, exhibit limited dynamic performance due to the viscoelastic properties of the polymer membrane. Several studies have used flexure structures as pre-stretching elements, but the overall design was neither compact nor small for use in micro robots [22], [23].

In this paper, we present the compliant microgripper using a novel miniaturized DEA. The actuator uses spiral flexure to pre-stretch the DEA membrane in a single direction. The proposed soft actuator has a compact and miniaturized structure (diameter: 10 mm) and can produce a large output force over 110 mN with high bandwidth. Using the proposed actuator, the microgripper was designed as shown in Fig. 1. By controlling the input voltage, we were able to control the proposed microgripper. We validate the performance of our compliant microgripper by demonstrating that it can grasp and manipulate various objects regardless of their shape and size.

II. Actuator Design and Working Principle

Here, we present a DEA-based soft actuator for microgripper that has a soft, lightweight, and small (diameter $<$10 mm) structure with high bandwidth. The design of the proposed actuator follows the basic concept of a double-cone DEA [13]. Among various DEA configurations, a double-cone DEA can produce high output force and displacement in a single direction [18]–[20]. The double-cone DEA is mainly composed of a passive elastomer layer, a dielectric elastomer (DE) layer, and an inner spacer, as in Fig. 2(a). A passive elastomer layer was used as a biasing element to achieve an antagonistic configuration and to apply pre-loading to the DE membrane. However, the viscoelasticity of the passive elastomer layer limits the dynamic response of the actuator. To enhance dynamic response, the proposed actuator uses a spiral flexure as a biasing element as shown in Fig. 2(a). Spiral flexures are composed of multiple spiral slots. Taking advantage of their thin (thickness: 0.1 mm), simple, and lightweight structure, spiral flexures have the potential to be fabricated with a small size. In addition, spiral flexure can be used as a linear spring which can produce a large stroke without a buckling problem and has a fast dynamic response [24]. The proposed actuator consists of a spiral flexure, an inner spacer, and a multi-layered DEA, as presented in Fig. 2(b). The actuation of the proposed actuator depends on the force balance exerted by a spiral flexure and a deformed DEA membrane. Without an input voltage, the restoring force exerted by the deformed DEA membrane (F_{DEA}) is balanced with the restoring force by spiral flexure ($F_{flexure}$). When the voltage is applied, the DEA membrane is compressed in the thickness direction due to an electrostatic pressure. This thickness compression leads to planar area expansion of the DEA membrane since the DE is an incompressible material [15]. Finally, the expansion of the DEA membrane causes the inner spacer to move downward until force balance is achieved.

III. Actuator Fabrication and Experiment

A. Fabrication of the actuator

The performance of the DEA highly depends on the selection of DE materials. For enhanced performance, the DE materials should have a low modulus, high dielectric constant, and high electrical breakdown strength [15]. Among various DEs, acrylic elastomer (3M VHB 4905) has high DE constant (4.53 @ 1Hz), low Young's modulus (0.4 MPa), and high dielectric strength (25 kV/mm @ 0.5 mm); however, it also has high viscoelasticity [15]. Due to its characteristic, it has been reported that acrylic-based DEA has benefits in generating large strain in low frequency range [15]. Since grippers mainly operate in the low frequency range ($<$1 Hz), acrylic elastomer was chosen as a DE material.

The overall fabrication process of the proposed actuator is summarized in Fig. 3. A 0.5 mm thick 3M VHB 4905 was bi-axially pre-stretched to a ratio of 4 and bonded to the 0.2 mm thick frame with an inner diameter of 6 mm, and outer diameter of 10 mm. Then multi-walled carbon

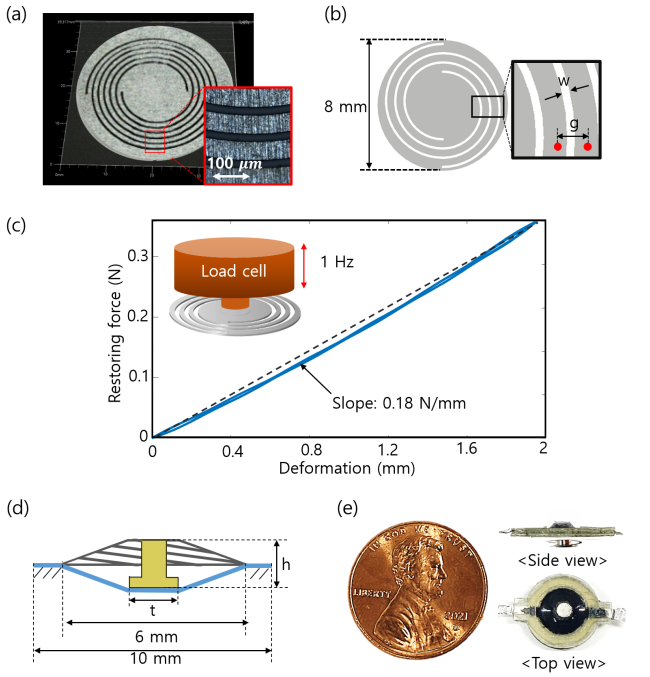

Fig. 4. (a) Captured image of the fabricated spiral flexure by chemical etching. (b) Design parameters of the spiral flexure. (c) Measured hysteresis loop of the fabricated spiral flexure at 1 Hz. (d) Design parameters of the proposed actuator. (e) Fabricated actuator.

TABLE I

DESIGN PARAMETERS OF THE PROPOSED ACTUATOR

Category	Parameters	Symbol	Value
Spiral flexure	Spiral gap	g	0.6 mm
	Spiral width	w	0.25 mm
Inner spacer	Spacer height	h	3 mm
	Spacer diameter	t	2.4 mm

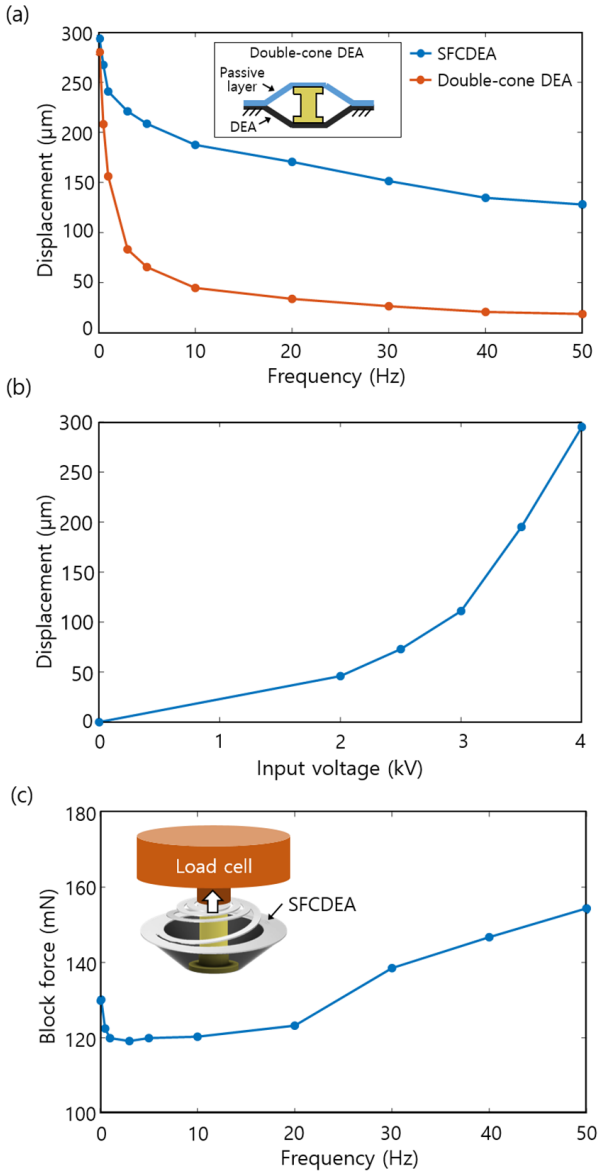

Fig. 5. Experimental results of the proposed actuator: (a) Comparison of the measured displacement profiles of the proposed actuator and double-cone DEA at 4kV. (b) Measured displacement of the actuator with input voltage changing at 0.1 Hz, and (c) measured block force profiles of the actuator with the input frequency at 4kV.

nanotubes (MWCTNs) were brushed on the both surface of DE membrane to form a compliant electrode. To make electrical connections, 50 μm thick aluminum tapes were attached to DE membrane. This process was repeated three times to fabricate a multi-layered DEA. The spiral flexure was made of 0.1 mm thick stainless steel (SUS304) sheet. The manufacturing process of the spiral flexure was done by the chemical etching process to achieve high fabrication precision. Fabrication process of the actuator was finalized by inserting an acrylic inner spacer between the multi-layered membrane and the spiral flexure.

The key point of the proposed actuator is using a miniaturized spiral flexure as a biasing element of the DEA. Therefore, the dynamic performance of the actuator is highly dependent on the dynamic response of the spiral flexure. To check the quality of the fabricated spiral flexure, 3D surface geometry, and the surface profile were captured by a 3D optical profiler (VR-5200, Keyence) and a microscope (Axio Scope A1, Zeiss), as seen in Fig. 4(a). Results showed that the spiral flexure can be fabricated with high precision by chemical etching process. The properties of the spiral flexure such as the spring constant can be controlled by two design parameters; spiral gap (g) and spiral width (w). The design parameters of the fabricated spiral are summarized in Fig. 4(b) and Table I. To evaluate the dynamic performance of the fabricated spiral flexure, the passive restoring force of the flexure was measured. In this experiment, the position of the load cell was controlled by using the linear stage. The linear stage was controlled to move a distance of 2 mm under a frequency of 1 Hz. Results are plotted in Fig. 4(c). Results showed that the spiral flexure exhibits high linearity between the displacement and the restoring force, with a

small hysteresis error of 1.7 %. This indicates that the spiral flexure can work as a linear spring with a spring constant of 0.18 N/mm. The overall design parameters of the actuator are summarized in Fig. 4(d) and Table I. Fig. 4(e) shows the fabricated actuator. The weight of the fabricated actuator was 0.2 g.

B. Performance Test of Actuator

The performance of the proposed actuator was evaluated by measuring the output displacement and the output force characteristics. For performance comparison, double cone DEA was fabricated with the same dimension of the fabricated actuator. The passive layer of the double-cone DEA was made of a multi-layered pre-stretched acrylic elastomer. During the experiment, actuators were mounted on top of the anti-vibration table. The input voltage was controlled by using a DAQ board (USB-6003, National instruments) and amplified by a high voltage amplifier (AMJ-4B10, Matsusada). We applied sinusoidal voltage signals with a frequency range of 0.1 to 50 Hz at 4 kV to the actuator. Simultaneously, the displacement of the proposed actuator was measured by a laser displacement sensor (LK-G3000, Keyence). Results are plotted along the frequency range as in Fig. 5(a). Results showed that the actuator can produce higher displacement than the double-cone DEA in the overall frequency range (0.1∼50 Hz). Both actuators have a maximum displacement at 0.1 Hz. The displacement of the double-cone DEA decreases sharply when the frequency of input voltage increases due to the high viscosity of the passive membrane. The calculated bandwidth of the double-cone DEA was around 0.6 Hz. Thanks to the elasticity of the spiral flexure, the proposed actuator has a higher bandwidth (5 Hz) than the double-cone DEA (0.6 Hz). The maximum output displacement of the actuator was 295 μm at the operating frequency of 0.1 Hz. In addition, results showed that the actuator can produce displacement over 130 μm at high frequency range (∼50 Hz). The output displacement of the actuator was measured while changing the input voltage at 0.1 Hz. The results indicate that the actuator can produce programmable output by controlling the input voltage, as in Fig. 5(b).

The dynamic performance of the actuator was further evaluated by observing the output force characteristics. The experiments were conducted in the same setup done in the displacement test. The load cell was placed on top of the actuator. The measured block force profiled of the actuator is plotted in Fig. 5(c). Results showed that the actuator can produce an output block force larger than 115 mN in all frequency ranges of 0.1 to 50 Hz. At 0.1 Hz, the measured block force was 130.1 mN. In addition, the measured block force exhibits a unique trend that gradually increasing after 3 Hz. This is likely owing to the resonance frequency of actuator due to the effect of the loading condition [21]. The results of the dynamic tests represent that the actuator can be used in various applications operating at both low frequencies and high frequencies (∼50 Hz).

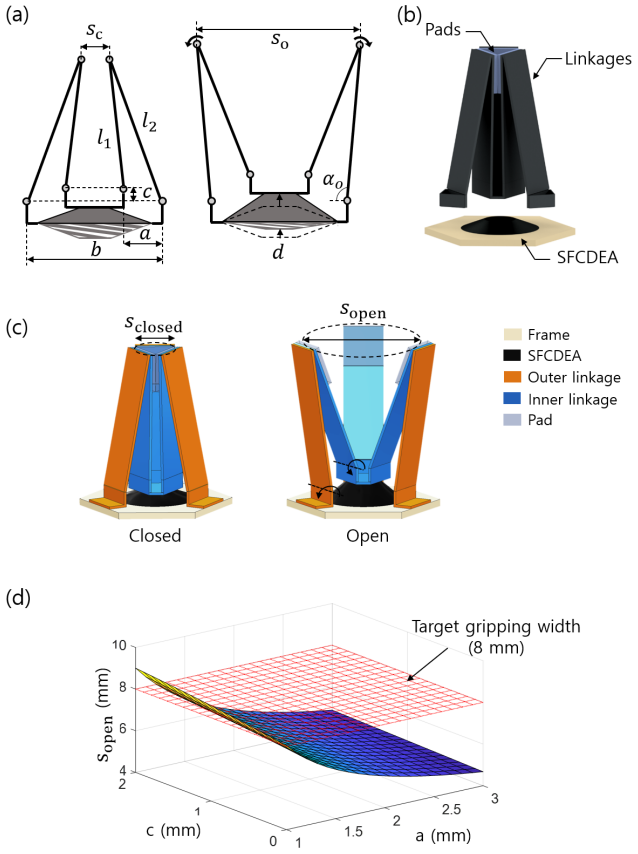

Fig. 6. (a) Illustration of the kinematic design and the working mechanism of the compliant microgripper. (b) Overall design concept of the microgripper. (c) Schematic representation of the detailed mechanical components. (d) Analysis of the maximum gripping width under different design parameters using the kinematics of the gripper.

IV. Compliant Microgripper

A. Performance Test of Actuator

In the previous section, we developed a soft actuator which has a small size (diameter: 10 mm), a thin structure (thickness: 3 mm) and a high bandwidth (∼5 Hz). Fabricated actuator can produce the output displacement more than 0.25 mm in the frequency range of 0.1 to 1 Hz. We designed the microgripper using the proposed actuator. The working principle and the kinematic design of the microgripper is illustrated in Fig. 6(a). The gripper is composed of the gripper linkage mechanism and the polymer actuator. The design of the gripper linkage can be modulated by five design parameters, as in Fig. 6(a). In the initial state, the gripper was designed to be in the closing state. The actuation of the polymer actuator connected to the gripper generates the opening motion. Thanks to the flexibility and the softness of the actuator, the microgripper can have a compliance that enables versatile and delicate grasping. The relation between the opening width of the gripper and the displacement output of the actuator is an important design consideration. This relationship can be derived by solving the kinematics equations of the gripper as follows:

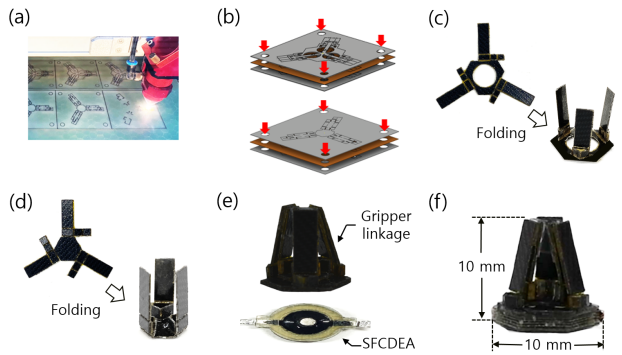

Fig. 7. Manufacturing process of the microgripper: (a) Laser cutting each layer. (b) Layers are aligned, laminated and bonded. (c) Cutting laminated outer linkage layer and folding, and (d) inner layer. (e) Assembling actuators and linkages. (f) Fabricated microgripper.

$$l_2 = \sqrt{\left(\sqrt{l_1^2 - \left(\frac{b}{2} - \frac{s_c}{2} - a\right)^2} + c\right)^2 + \left(\frac{b}{2} - \frac{s_c}{2}\right)^2} \quad (1)$$

$$\alpha_o = \tan^{-1}\left(\frac{c+d}{a}\right) + \cos^{-1}\left(\frac{l_2^2 + (c+d)^2 + a^2 - l_1^2}{2l_2\sqrt{a^2 + (c+d)^2}}\right) \quad (2)$$

$$s_o = b - 2l_2 \cos\alpha_0 \quad (3)$$

where l_1 is the inner linkage length, l_2 is the outer linkage length, a is the inner gap, b is the outer diameter, c is the height gap, d is the output displacement of the actuator, s_c is the minimum gripping width, s_o is the maximum gripping width, and α_o is the inner angle as shown in Fig. 6(a).

The compliant microgripper was designed following a kinematic model, as shown in Fig. 6(b). The three-finger gripper design allows the gripper to have a delicate and powerful gripping performance. Smart composite microstructure (SCM) technology was used to fabricate the linkage mechanism due to its macroscale manufacturing capability [25]. Rubber pads were mounted on the finger to provide strong gripping force. Fig. 6(c) describes the mechanical components of the gripper in a detail. Actuation of the polymer actuator moves the inner linkage upward. The vertical motion of the inner linkage is then converted to rotary motion, which leads the opening motion of the gripper. The main design target of the gripper was to have a maximum gripping width (s_o) larger than 8 mm at opening state. In addition, considering three-finger gripper design as shown in Fig. 6(c), the minimum gripping width of the gripper (s_c) was set as 3 mm. Then the design parameters of the gripper were selected to satisfy these requirements. Fig. 6(d) shows the calculated maximum gripping width under different parameters using (1)–(3). The displacement of the actuator was assumed as 0.25 mm. Table II summarized the determined design parameters of the microgripper.

The manufacturing steps of the microgripper is illustrated in Fig. 7. The rigid links of the origami mechanism were made of 100 μm thick fibereglass sheets and compliant joints were made of 12.5 μm thick polyimide film (Kapton, Dupont). 12.5 μm thick acrylic bonding sheet was used to bond each layer. Each layer was micromachined by a laser into the designed pattern. The layers were aligned using dowel pins and bonded. The assembled laminated layers were cut along the line, and folded as in Fig. 7(c). Outer linkage and inner linkage are then assembled via adhesive (Locite 401, Henkel). The manufacturing process is finalized by bonding the assembled linkages and proposed actuator as shown in Fig. 7(e). Fabricated microgripper is shown in Fig. 7(f). The gripper has a dimension of 10 × 10 × 10 mm^3 and a weight of 0.36 g.

TABLE II
DESIGN PARAMETERS OF THE MICROGRIPPER

Parameters	Symbol	Value
Inner linkage length	l_1	10 mm
Outer linkage length	l_2	11.17 mm
Inner gap	a	1 mm
Outer diameter	b	8 mm
Height gap	c	1 mm

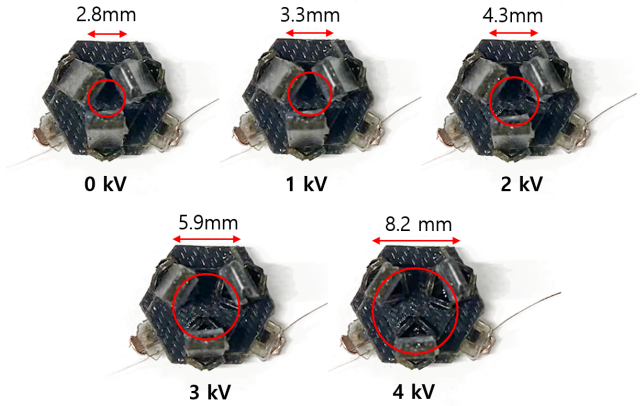

Fig. 8. Captured image of the actuation of the microgripper with various input voltage.

B. Experimental Evaluation and Demonstration

The fabricated microgripper was evaluated by observing the gripping width under various input voltage. The images of the fabricated gripper were captured with 0 to 4 kV input voltage and shown in Fig. 8(a). During the test, DC input voltage was applied to the gripper. Under zero voltage, the gripper has initial gripping width of 2.8 mm. By modulating the input voltage, the gripping width can be controlled. Under 4 kV input voltage, the gripper shows maximum gripping width of 8.2 mm. Results showed that the fabricated gripper satisfies the design target (gripping width: 8 mm). Then, the fabricated microgripper was used to demonstrate the picking-and-placing of various small sized objects. The gripper demonstrated successful gripping and manipulation of both a soft ball (diameter of 3.2 mm, weight of 0.1 g), a rigid weight (diameter of 5 mm, weight of 5 g) and a

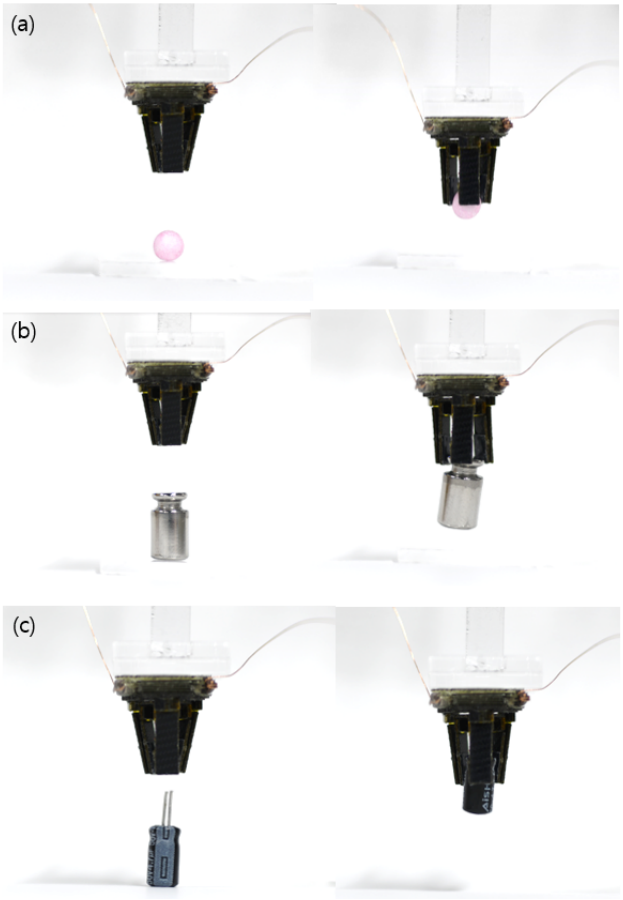

Fig. 9. Gripper shown gripping various objects: (a) A soft ball, (b) a rigid weight, and (c) electrical component.

small electrical component (diameter of 6.2 mm, weight of 0.6 g). Results showed that the gripper enables gripping and manipulating a heavy object (payload-to-weight ratio of 14). In addition, the high bandwidth of the proposed actuator enable gripper to produce fast gripping motion. We validated the microgripper enables gripping both soft and rigid objects without the needs for complex control algorithm or sensory feedback owing to its compliance. The gripper performance is shown in Fig. 9. The demonstration indicates the feasibility of gripping various objects regardless of their shape with safe interaction.

V. Conclusion

In this paper, we present the design, fabrication and demonstration of the compliant microgripper driven by a soft polymer actuator. The proposed actuator follows the basic concept of the double-cone DEA, but uses spiral flexure as a biasing element of DEA membrane. In this design, the spiral flexure has several strengths. First, spiral flexure has a thin, a compact structure and a can be manufactured at small scale by chemical etching process. In addition, spiral flexure has a characteristic of a linear spring which can produce large stroke without a buckling. The polymer actuator was fabricated with dimensions of $10 \times 10 \times 3$ mm^3, and a weight of 0.2 g. The actuator was capable of producing a maximum displacement of 0.29 mm at 0.1 Hz under 4 kV input voltage. Measured bandwidth of the actuator was 5 Hz. The actuator provide an output block force larger than 115 mN in the frequency range of 0.1 to 50 Hz. Using the proposed actuator, we designed and fabricated the microgripper. The gripper can be manufactured at the millimeter scale ($10 \times 10 \times 10$ mm^3) by using laminated design and SCM technology. Based on the kinematics model of the gripper, the gripper was designed to have a maximum gripping width larger than 8 mm. We successfully demonstrated the microgripper enables gripping various small size objects without a sensory feedback due to its compliance.

Our future work will cover an optimization of the actuator by deriving a dynamic model. Based on the optimization, the dynamic performances of the gripper can be enhanced. Further consideration of the gripping force capability of the microgripper will be also discussed in the future. Although we designed the microgripper focusing on the gripping width, the gripping force capability is a key factor.

References

[1] R. Zhang, J. Chu, H. Wang, and Z. Chen, "A multipurpose electrothermal microgripper for biological micro-manipulation", *Microsyst. Technol.*, vol. 19, pp. 89-97, Jan. 2013.

[2] Z. Lyu and Q. Xu, "Recent design and development of piezoelectric-actuated compliant microgrippers: A review", *Sens. Actuator A Phys.*, vol. 331, pp. 113002, Nov. 2021.

[3] F. Wang, C. Liang, Y. Tian, X. Zhao, and D. Zhang, "Design and Control of a Compliant Microgripper With a Large Amplification Ratio for High-Speed Micro Manipulation", *IEEE/ASME Trans. Mechatron.*, vol. 21, pp. 1262-1271, Jan. 2016.

[4] H. Mehrabi, M. Hamedi, and I. Aminzahed, "A novel design and fabrication of a micro-gripper for manipulation of micro-scale parts actuated by a bending piezoelectric", *Microsyst. Technol.*, vol. 26, pp. 1563-1571, Dec. 2019.

[5] G. Shao, H. O. T. Ware, J. Huang, R. Hai, L. Li, and C. Sun, "3D printed magnetically-actuating micro-gripper operates in air and water", *Addit. Manuf.*, vol. 38, pp. 101834, Feb. 2021.

[6] S. Kodera, T. Watanabe, Y. Yokoyama, and T. Hayakawa, "Microgripper Using Soft Microactuators for Manipulation of Living Cells", *Micromachines*, vol. 13, pp. 794, May 2022.

[7] J. H. Kyung, B. G. Ko, Y. H. Ha, and G. J. Chung, "Design of a microgripper for micromanipulation of microcomponents using SMA wires and flexible hinges", *Sens. Actuator A Phys.*, vol. 141, pp. 144-150, Jan. 2008.

[8] J. H. Kyung, B. G. Ko, Y. H. Ha, and G. J. Chung, "Design of a microgripper for micromanipulation of microcomponents using SMA wires and flexible hinges", *Sens. Actuator A Phys.*, vol. 141, pp. 144-150, Jan. 2008.

[9] T. N. Do, H. Phan, T.-Q. Nguyen, and Y. Visell, "Miniature Soft Electromagnetic Actuators for Robotics Applications', *Adv. Funct. Mater.*, vol. 28, pp. 1800244, Mar. 2018.

[10] A.F. Alogla, F. Amalou, C. Balmer, P. Scanlan, W. Shu, and R. L. Reuben, "Micro-tweezers: Design, fabrication, simulation and testing of a pneumatically actuated micro-gripper for micromanipulation and microtactile sensing", *Sens. Actuator A Phys.*, vol. 236, pp. 394-404, July 2015.

[11] Y. Roh, M. Kim, S. M. Won, D. Lim, I. Hong, S. Lee, T. Kim, C. Kim, D. Lee, S. Im, G. Lee, D. Kim, D. Shin, D. Gong, B. Kim, S. Kim, S. Kim, H. K. Kim, B.-K. Koo, S. Seo, J.-S. Koh, D. Kang, and S. Han, "Vital signal sensing and manipulation of a microscale organ with a multifunctional soft gripper", *Sci. Robot.*, vol. 6, pp. eabi6774, Oct. 2021.

[12] M. Boyvat, J.-S. Koh, and R. J. Wood, "Addressable wireless actuation for multijoint folding robots and devices", *Sci. Robot.*, vol. 2, pp. eaan1544, July 2017.

[13] C.-J. Peng, L. Seurre, E. Cattan, G. T.-M. Nguyen, C. Plesse, L. Chassagne, and B. Cagneau, "Toward an Electroactive Polymer-Based Soft Microgripper", *IEEE Access*, vol. 9, pp. 32188-32195, Feb. 2021.

[14] H. R. Cheong, C. Y. Teo, P. L. Leo, K. C. Lai, and P. S. Chee, "Wireless-powered electroactive soft microgripper", *Smart Mater. Struct.*, vol. 27, pp. 055014, Apr. 2018.
[15] J.-H. Youn, S. M. Jeong, G. Hwang, H. Kim, K. Hyeon, J. Park and K.-U. Kyung, "Dielectric elastomer actuator for soft robotics applications and challenges" *Appl. Sci.*, vol. 10, no. 2, p. 640, Jan. 2020.
[16] J. Shintake, S. Rosset, B. Schubert, D. Floreano, and H. Shea, "Versatile Soft Grippers with Intrinsic Electroadhesion Based on Multifunctional Polymer Actuator", *Adv. Mater.*, vol. 28, pp. 231-238, Nov. 2015.
[17] G. Hwang, J. Park, D.S.D. Cortes, K. Hyeon, and K.-U. Kyung, "Electroadhesion-Based High-Payload Soft Gripper With Mechanically Strengthened Structure", *IEEE Trans. Ind. Electron.*, vol. 69, pp. 642-651, Jan. 2021.
[18] C. Cao and A. T. Conn, "Performance Optimization of a Conical Dielectric Elastomer Actuator", *Actuators*, vol. 7, pp. 32, June 2018.
[19] C. Cao, S. Burgess, and A.T. Conn, "Toward a Dielectric Elastomer Resonator Driven Flapping Wing Micro Air Vehicle", *Front. Robot. AI*, vol. 5, pp. 137. Jan. 2019.
[20] J.-H. Youn, I. B. Yasir, and K.-U. Kyung, "Self-sensing Soft Tactile Actuator for Fingertip Interaction", in *IEEE/RSJ International Conference on Intelligent Robots and Systems (IROS)*, Las Vegas, USA, 2020, pp. 8939-8944.
[21] J.-H. Youn, H. Mun, and K.-U. Kyung, "A Wearable Soft Tactile Actuator with High Output Force for Fingertip Interaction", *IEEE Access*, vol. 9, pp. 30206-30215, Feb. 2021.
[22] G. Berselli, R. vertechy, G. Vassura, and V. Parenti-Castelli, "Optimal Synthesis of Conically Shaped Dielectric Elastomer Linear Actuators: Design Methodology and Experimental Validation", *IEEE/ASME Trans. Mechatron.*, vol. 16, pp. 67-79, Feb. 2011.
[23] F. A. M. Ghazali, C. K. Mah, A. AbuZaiter, P. S. Chee, and M.S. Mohamed Ali, "Soft dielectric elastomer actuator micropump", *Sens. Actuator A Phys.*, vol. 263, pp. 276-284, June 2017.
[24] N. Chen, X. Chen, Y. N. Wu, C. G. Yang, and L. Xu, "Spiral profile design and parameter analysis of flexure spring", *Cryogenics*, vol. 46, pp. 409-419, June 2006.
[25] R. J. Wood, S. Avadhanula, R. Sahai, E. Steltz, and R. S. Fearing, "Microrobot Design Using Fiber Reinforced Composites", *J. Mech. Design*, vol. 130, pp. 052304, May 2008.